# Power Deposition of a Microstrip Applicator Radiating into a Layered Biological Structure

LUC BEYNE AND DANIEL DE ZUTTER

*Abstract* — **The power deposited by a microstrip antenna into a layered biological structure is investigated. The solution is based on an integral equation for the surface current density on the antenna and on an electric Green's dyadic for the fields inside a planar stratified medium. The integral equation is solved using the method of moments in conjunction with the point-matching technique. The modeling of the surface current takes the edge conditions into account. Special attention is devoted to a correct modeling of the excitation of the antenna by a coaxial feed. The numerical results focus on the power deposition as a function of depth.**

## I. Introduction

MICROSTRIP ANTENNAS are used in a broad range of applications and discussed in a large amount of technical literature and books (see e.g. [1]). For the design and analysis of microstrip antennas, a number of authors start from *a priori* knowledge of the behavior of the fields in parts of space [2]–[5]. This results in a reduction of the volume that must be covered by the calculations. Much interest is also devoted to special geometries of microstrip antennas and to resonant modes of the structures under study [6]–[10].

A relatively new application is the use of microstrip antennas in the hyperthermia treatment of cancer [2], [10], [11]. In this particular application, interest is focused on the power deposition inside a biological tissue. This necessitates a correct evaluation of the surface current on the microstrip patch excluding simplified methods starting from an educated guess of the current distribution. The method also must be able to calculate the near fields correctly and should allow for arbitrarily shaped patches. To simplify the problem, the biological tissue will be modeled as a two-dimensional multilayered structure.

In [2] a coupled integral equation technique is proposed to analyze the radiation of a microstrip antenna. The method is approximate as it neglects part of the exciting current and in the case of a multilayered structure the number of coupled equations would become too large to handle.

Manuscript received April 11, 1987; revised August 28, 1987. This work was supported in part by the National Fund for Scientific Research of Belgium

L. Beyne was with the Laboratory of Electromagnetism and Acoustics, University of Ghent, Belgium. He is now with Alcatel Bell Telephone, Antwerp, Belgium

D. De Zutter is with the Laboratory of Electromagnetism and Acoustics, University of Ghent, Ghent, Belgium.

IEEE Log Number 8717905.

In [11] a mixed-potential approach is proposed in conjunction with the method of moments with rooftop basis functions. This analysis focuses on resonant behavior and radiation patterns.

Our approach is based on an integral equation for the surface current. The derivation of the relevant electric Green's dyadic suited for this purpose has been presented elsewhere [12]. Our basis functions take the singular behavior of the current components at the edges of the microstrip patch into account. Special attention is also given to a correct modeling of the excitation. The numerical results focus on the power deposition inside the biological tissue. The method allows a rather fast evaluation of the fields at every point of space once the unknown surface current on the microstrip antenna has been determined.

## II. General Formulation of the Problem

We consider the general structure shown in Fig. 1. The microstrip patch resides at the interface of the microstrip substrate and the first layer of a planar stratified medium. This medium will be used as a model of a layered biological tissue. The patch is coaxially fed and a total current $I$ is flowing onto the surface of the patch at $O$. The fields generated by the radiating microstrip antenna depend upon the unknown surface current distribution $\bar{J}_S$. The electric field depends upon $\bar{J}_S$ through the electric Green's dyadic $\bar{\bar{G}}_e$:

$$\bar{E}(\bar{r}) = \iint_S \bar{\bar{G}}_e(\bar{r}|\bar{r}') \cdot \bar{J}_S(\bar{r}')\, dS'. \tag{1}$$

The integration extends over the surface of the antenna. The position vector $\bar{r}$ belongs to an observation point, and $\bar{r}'$ belongs to a variable integration point on the surface of the patch.

A first step in solving the problem is the determination of the Green's dyadic $\bar{\bar{G}}_e$. In [12] it is shown that $\bar{\bar{G}}_e$ can be derived from a scalar Green's function problem and that a numerically accurate procedure makes the calculation of this Green's function possible for layered structures with high losses and/or many layers. The method proposed in [12] is also suitable if the observation point $\bar{r}$ is located in the source region, i.e., on the microstrip patch itself.

Starting from (1), we arrive at an integral equation for the surface current density $\bar{J}_S$ by expressing the fact that the tangential electric field must be zero on the microstrip

0018-9480/88/0100-0126$01.00 

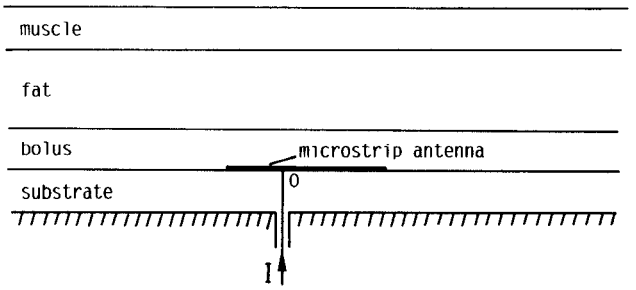


Fig. 1. Microstrip antenna radiating into a layered biological structure.

patch. This leads to

$$E_x(\bar{r}_S) = \iint_S \left[ G_{exx}(\bar{r}_S|\bar{r}')J_{Sx}(\bar{r}') + G_{exy}(\bar{r}_S|\bar{r}')J_{Sy}(\bar{r}') \right] dS' = 0$$

$$E_y(\bar{r}_S) = \iint_S \left[ G_{eyx}(\bar{r}_S|\bar{r}')J_{Sx}(\bar{r}') + G_{eyy}(\bar{r}_S|\bar{r}')J_{Sy}(\bar{r}') \right] dS' = 0 \quad (2)$$

where $\bar{r}_S$ is located on the patch. Strictly speaking, (2) is obtained by a limiting process in which $\bar{r}_S$ approaches the surface. This limiting procedure will be important in the sequel.

*Discretization of the Surface Current*

The method of moments is a well-known technique for solving an integral equation of the type given in (1). In the sequel, the unknown surface current will be modeled by a finite number of basis functions and by special functions (the excitation functions) to accurately model the excitation by the current $I$. On the microstrip antenna, $\bar{J}_S$ can be written as

$$\bar{J}_S(\bar{r}') = \sum_{i=1}^{N} \left[ j_{xi} f_{xi}(\bar{r}')\bar{u}_x + j_{yi} f_{yi}(\bar{r}')\bar{u}_y \right] + \left[ g_x(\bar{r}')\bar{u}_x + g_y(\bar{r}')\bar{u}_y \right] \quad (3)$$

where $f_{xi}(\bar{r}')$ and $f_{yi}(\bar{r}')$ represent the $N$ basis functions and $g_x$ and $g_y$ are the excitation functions. The complex constants $j_{xi}$ and $j_{yi}$ will be determined by requiring that (2) be satisfied in $N$ points $r_{Sk}$, $k = 1,2,\cdots,N$ of the antenna. This approach is the well-known point-matching technique. The above formulation leads to the solution of the following set of $2N$ linear equations with $2N$ unknowns:

$$\sum_{i=1}^{N} j_{xi} m_{xxki} + \sum_{i=1}^{N} j_{yi} m_{xyki} = b_{xk}$$

$$\sum_{i=1}^{N} j_{xi} m_{yxki} + \sum_{i=1}^{N} j_{yi} m_{yyki} = b_{yk} \quad (4)$$

where

$$m_{\alpha\beta ki} = \iint_S G_{e\alpha\beta}(\bar{r}_{Sk}|\bar{r}')f_{\beta i}(\bar{r}')\, dS' \quad (5)$$

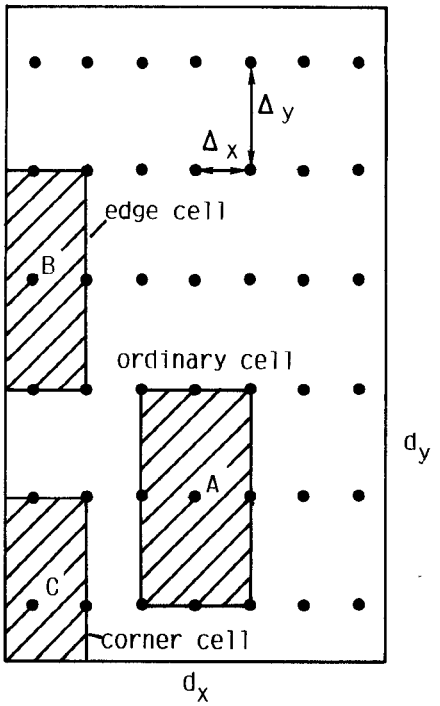


Fig. 2 Discretization of the surface current density.

and

$$b_{\alpha k} = -\iint_S \left[ G_{e\alpha k}(\bar{r}_{Sk}|\bar{r}')g_x(\bar{r}') + G_{e\alpha y}(\bar{r}_{Sk}|\bar{r}')g_y(\bar{r}') \right] dS' \quad (6)$$

with $\alpha = x,\ y$; $\beta = x,\ y$ and $k,\ i = 1,2,\cdots,N$.

## III. Solution for a Rectangular Patch

In the sequel our attention will be focused on the rectangular microstrip patch. Our approach is based on a grid of rectangular cells. If the dimensions of the patch are $d_x$ and $d_y$, we divide the patch in $N_x$ by $N_y$ cells. We consider three kinds of elementary basis functions and their center points $A$, $B$, and $C$ as indicated in Fig. 2: ordinary cells, edge cells, and corner cells. These functions only differ from zero over a limited part of the surface, as indicated by the shaded areas. Their value depends only upon the distance to the center point $\bar{r}_c$ ($A$, $B$, and $C$ in Fig. 2). We also require these functions to be continuously differentiable to ensure that the surface charge density remains continuous. For an ordinary cell the above requirements lead to

$$f_{xi}(\bar{r}) = f_{yi}(\bar{r}) = \phi_{x1}(x - x_c)\phi_{y1}(y - y_c) \quad (7)$$

where

$$\begin{aligned} \phi_{x1}(x) &= 1 - (32/7)\tau^2, && 0 \leqslant \tau \leqslant 1/8 \\ &= 15/14 - (8/7)\tau, && 1/8 \leqslant \tau \leqslant 7/8 \\ &= (32/7)(\tau - 1)^2, && 7/8 \leqslant \tau \leqslant 1 \end{aligned} \quad (8)$$

where $\tau = |x|/\Delta_x$. The function $\phi_{y1}(y)$ is defined in an analogous way and $\Delta_x$ and $\Delta_y$ are shown in Fig. 2.

In the cells near the edge and in the corners, $f_{xi}$ and $f_{yi}$ cannot be chosen in the same way due to the behavior of

the surface current near the edge. The component of the current parallel to the edge becomes singular as $1/\sqrt{d}$, where $d$ is the distance to the edge [13]. The component of the current perpendicular to the edge becomes zero as $\sqrt{d}$. Our model takes these phenomena into account. For a cell at the left edge of the patch (see Fig. 2), we write

$$f_{yl}(\bar{r}) = \phi_{x2}(x)\phi_{y1}(y - y_c)$$
$$f_{xl}(\bar{r}) = \phi_{x3}(x)\phi_{y1}(y - y_c) \tag{9}$$

where $\phi_{y1}$ was given above and where $\phi_{x2}$ and $\phi_{x3}$ are

$$\begin{aligned}
\phi_{x2}(x) &= \phi_{x1}(x - \Delta_x/2), && 1/2 < \kappa \\
&= 1 + (64/11)(\kappa - 1/2)^2, && 3/8 < \kappa < 1/2 \\
&= (3/11)(6/\kappa)^{1/2}, && 0 < \kappa < 3/8 \\
\phi_{x3}(x) &= \phi_{x1}(x - \Delta_x/2), && 1/2 < \kappa \\
&= 1 - (64/13)(\kappa - 1/2)^2, && 3/8 < \kappa < 1/2 \\
&= (8/13)(6\kappa)^{1/2}, && 0 < \kappa < 3/8
\end{aligned} \tag{10}$$

where $\kappa = x/\Delta_x$. The first equation in (9) models the current parallel to the edge; the second one models the current perpendicular to the edge.

Finally, we indicate how a corner cell (see Fig. 2) can be modeled by giving the result for the cell in the lower left corner:

$$f_{yl}(\bar{r}) = \phi_{x2}(x)\phi_{y3}(y)$$
$$f_{xl}(\bar{r}) = \phi_{x3}(x)\phi_{y2}(y). \tag{11}$$

The functions $\phi_{x2}$ and $\phi_{x3}$ were defined before and $\phi_{y2}$ and $\phi_{y3}$ are defined in an analogous way.

## IV. Modeling of the Input Current

The total current $I$ flowing onto the surface of the patch at O (see Fig. 1) gives rise to a radially divergent $1/r$ surface current density in the immediate neighborhood of the feed point, where $r$ represents the distance to this feed point. The excitation functions $g_x$ and $g_y$ are chosen such that they can model this behavior. In a small area around the feed point, they must remain zero in order to take the radius of the central conductor of the coaxial cable into account. As before, we require that the excitation functions be zero outside their definition region, but the transition between the $1/r$ divergence and the region where the excitation functions decay and finally become zero must be sufficiently smooth. Taking the above considerations into account, we choose the excitation functions to be

$$g_x(\bar{r})\bar{u}_x + g_y(\bar{r})\bar{u}_y = I(\bar{r} - \bar{r}_{\text{feed}})\phi_{\text{exc}}(\bar{r} - \bar{r}_{\text{feed}}) \tag{12}$$

where

$$\begin{aligned}
\phi_{\text{exc}}(\bar{r}) &= 0, && r < R_{\text{coax}} \\
&= 1/r^2, && R_{\text{coax}} \leq r \leq (7/16)R_{\max} \\
&= [2/r - (16/7R_{\max})][16/(7R_{\max})], && 7/16 \leq r/R_{\max} \leq 3/4 \\
&= 2(16/7)^2(r - R_{\max})^2/(R_{\max}^3 r), && 3/4 \leq r/R_{\max} \leq 1.
\end{aligned} \tag{13}$$

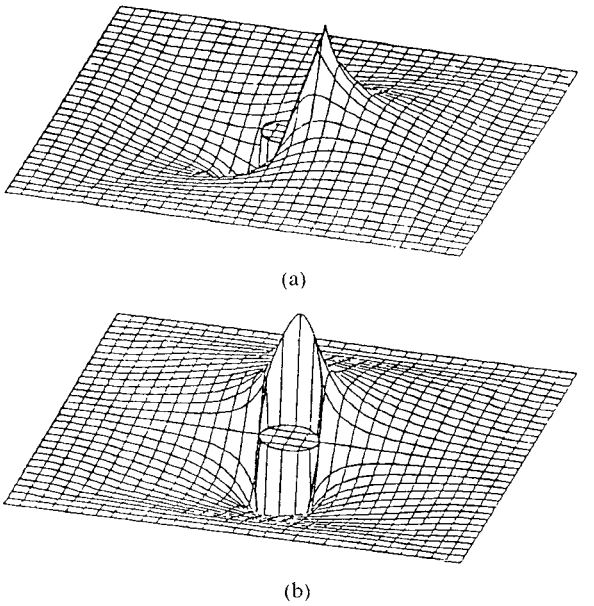

Fig. 3. Modeling of the excitation by a coaxial feed. (a) Excitation function $g_x$. (b) Excitation function $g_y$.

The area in which the excitation functions differ from zero is determined by $R_{\max}$ and the radius of the inner conductor of the coaxial cable by $R_{\text{coax}}$. We have chosen $R_{\max}$ in such a way that the excitation functions only differ from zero in a rectangular area of $3\Delta_x$ by $3\Delta_y$ around the feed point. Fig. 3 gives an impression of the variation of $g_x$ and $g_y$.

## V. Self-Patch Contributions

The calculation of the $m$ and $b$ elements in (5) and (6) is crucial to the solution of the discretized integral equation. The necessary integration over the surface $S$ of the microstrip antenna can be carried out numerically over the larger part of $S$, using a Gaussian quadrature formula. However, in the immediate vicinity of an observation point or point-matching point $\bar{r}_{Sk}$, the so-called self-patch contribution must be determined analytically. To that purpose we exclude a small rectangular surface $\sigma$ from $S$. This rectangle is centered around $\bar{r}_{Sk}$. As shown in [12], the Green's dyadic $\bar{\bar{G}}_e$ consists of a numerical part and an analytical part. For the self-patch contribution, only the analytical part is important as the integral involving the numerical part does not exhibit any singularities when source point and observation point coincide.

The above considerations allow us to formulate the problem for the $m$ elements in (5) as follows:

$$\begin{aligned}
m_{\alpha\beta kl} = &\iint_S \left[G_{e\alpha\beta}(\bar{r}_{Sk}|\bar{r}')\right]_{\text{num}} f_{\beta l}(\bar{r}')\, dS' \\
&+ \iint_{S-\sigma} \left[G_{e\alpha\beta}(\bar{r}_{Sk}|\bar{r}')\right]_{\text{ana}} f_{\beta l}(\bar{r}')\, dS' \\
&+ \iint_{\sigma} \left[G_{e\alpha\beta}(\bar{r}_{Sk}|\bar{r}')\right]_{\text{ana}} f_{\beta l}(\bar{r}')\, dS'.
\end{aligned} \tag{14}$$

Only the last integral in (14) must be calculated analytically. The numerical calculations of the other integrals

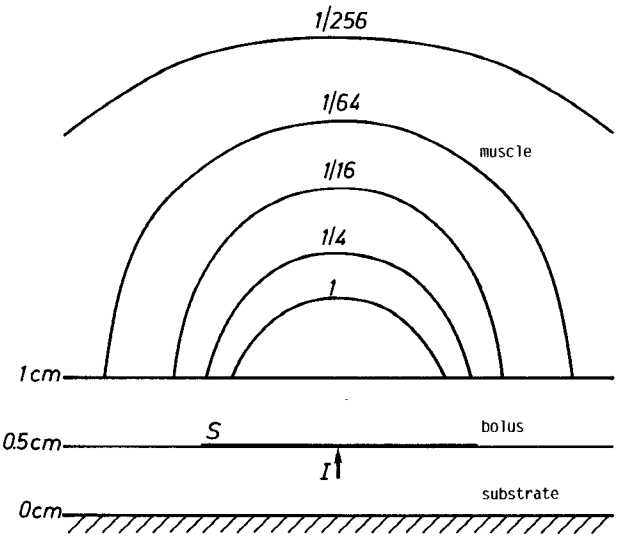


Fig. 4. Power deposition of a rectangular microstrip antenna in a bolus–muscle configuration

presents no difficulty. An analogous reasoning applies to the $b$ elements in (6).

In the neighborhood of each point $\bar{r}_{Sk}$ the functions $f_{\beta l}$, $\beta = x, y$, can be written as

$$f_{\beta l}(\bar{r}') = B_{00} + B_{20}\xi^2 + B_{02}\eta^2 + B_{22}\xi^2\eta^2. \tag{15}$$

The value of the $B$ coefficients follows directly from the definitions of the basis functions in (7)–(11), and $\eta = 0$, $\xi = 0$ represents the center of the rectangular patch $\sigma$. The Green's dyadic $\bar{\bar{G}}_e$ with its four elements $G_{e\alpha\beta}$, $\alpha = x, y$, $\beta = x, y$, has the form

$$\begin{vmatrix} W_0^e(\rho, z \to d_1) - W_2^e(\rho, z \to d_1)\cos 2\theta & -W_2^e(\rho, z \to d_1)\sin 2\theta \\ -W_2^e(\rho, z \to d_1)\sin 2\theta & W_0^e(\rho, z \to d_1) + W_2^e(\rho, z \to d_1)\cos 2\theta \end{vmatrix} \tag{16}$$

where $(\bar{r}_{Sk} - \bar{r}') = \rho(\cos\theta\bar{u}_x + \sin\theta\bar{u}_y)$. The variable integration point which covers $\sigma$ is $\bar{r}'$. The general expressions for the $W$ integrals are given in [12]. For the calculation of the self-patch contribution, the analytical parts of those $W$ integrals are important. The general results in [12] lead to

$$\begin{aligned} 4\pi(x^2+\rho^2)^{1/2}(W_0^e)_{\text{ana}} &= A - (B+C) \\ &\quad \cdot\left[(x^2+\rho^2)^{1/2} - x\right]^2\rho^{-2} \\ 4\pi(x^2+\rho^2)^{5/2}(W_2^e)_{\text{ana}} &= A(2x^2-\rho^2) - 3(B-C)\rho^2 \end{aligned} \tag{17}$$

where

$$\begin{aligned} &x = (z - d_1) \qquad A = \epsilon_0/(\epsilon_1+\epsilon_2) \\ &B = \left(\mu_1\epsilon_1^2 + \mu_2\epsilon_2^2\right)\Big/\left[(\epsilon_1+\epsilon_2)^2\mu_0\right] \qquad C = \mu_1\mu_2/(\mu_1+\mu_2). \end{aligned} \tag{18}$$

Here $\epsilon_i = \epsilon_0\epsilon_{ri} + \sigma_i/j\omega$ and $\mu_i$ represent, respectively, the complex permittivity and the magnetic permeability of the microstrip substrate ($i = 1$) and of the layer immediately above the microstrip antenna ($i = 2$).

It must be emphasized that the limit $z \to d_1$ or $x \to 0$ has been carefully retained. It can be seen that it is not always allowed to interchange the integration process in the self-patch integral over $\sigma$ and the limiting process $z \to d_1$. In order to evaluate the self-patch integrals correctly, it is necessary to start from the values (17) of the analytical parts of the $W$ integrals for $x \neq 0$. In a second step, the self-patch integrals are calculated with $x \neq 0$ and the limit $x \to 0$ is only applied to the result of that integration.

We will not go into further details here. With the above procedure the self-patch integrals for the $m$ elements in (5) and (14) can be found. The same procedure applies to the $b$ elements in (6). The actual integration always reduces to one of the following integrals:

$$\int f(\phi)\sin^q\phi/\cos^{q-p+2}\phi\, d\phi, \qquad q = 0, 2 \text{ and } p = 1, 3 \tag{19}$$

with $f(\phi) = 1$, $\sin 2\phi$, or $\cos 2\phi$.

## VI. Power Deposition of a Rectangular Microstrip Antenna

The approach followed in this paper aimed at calculating the radiation of a microstrip antenna in a layered lossy medium. This situation is of particular importance for the modeling of the hyperthermia treatment of cancer. In this section we will discuss a single example to illustrate the proposed method. More extensive numerical data will be provided in a future publication.

A relevant example is shown on Fig. 4. The microstrip antenna measures 2 cm by 2 cm; the excitation is at the center and the frequency is 915 MHz, a typical hyperthermia frequency. A first layer of 0.5 cm is the substrate of the microstrip antenna with $\epsilon_r = 2.53$ (Rexolit). The second layer is the water-bolus, 0.5 cm thick and with $\epsilon_r = 80$. This bolus must prevent the overheating of the tissue close to the microstrip antenna. The third layer is unbounded and represents muscle tissue with a complex permittivity $\epsilon_r = 58 - j12$. All the materials involved are nonmagnetic.

The surface current distribution generated on the antenna is shown on Fig. 5. The top drawing gives the in-phase components, the bottom drawing the quadrature components on a scale 100 times larger. Hence, the quadrature components are small compared with the in-phase ones.

The most important feature of the microstrip antenna is the distribution of the power generated inside the biological tissue. This distribution can be calculated starting from (1) when the surface current density is known. As the observation point $\bar{r}$ now lies everywhere in space, the full

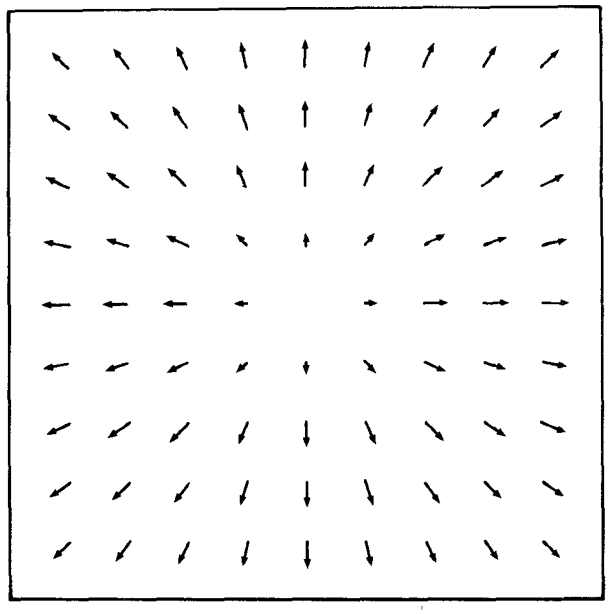

(a)

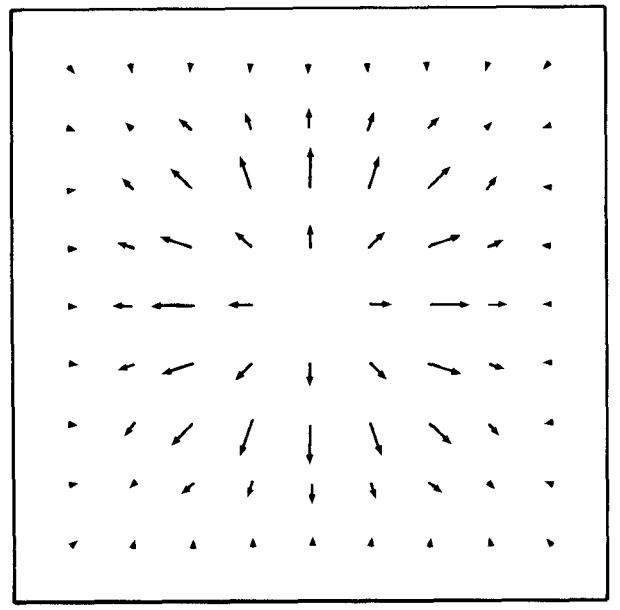

(b)

Fig. 5. (a) In-phase component of the surface current density relevant to the example of Fig. 4. (b) Quadrature component of the surface current density relevant to the example of Fig. 4.

Green's dyadic $\overline{\overline{G}}_e$ with its nine elements [12] must be taken into account. The power distribution in the muscle tissue is shown in Figs. 4 and 6. The labeled curves on Fig. 4 indicate how fast this dissipated power decays. Every curve is a contour of constant power corresponding to a value four times lower compared with the previous curve.

Fig. 6 gives results in a 4 cm by 4 cm area centered around the antenna but at several distances from the antenna, ranging from $z = 1$ cm, which is at the bolus–muscle interface, up to $z = 4$ cm. This result dramatically illustrates the defocusing of the power as the distance from the antenna increases. In a recent paper, Bardati *et al.* [14] found an analogous defocusing effect

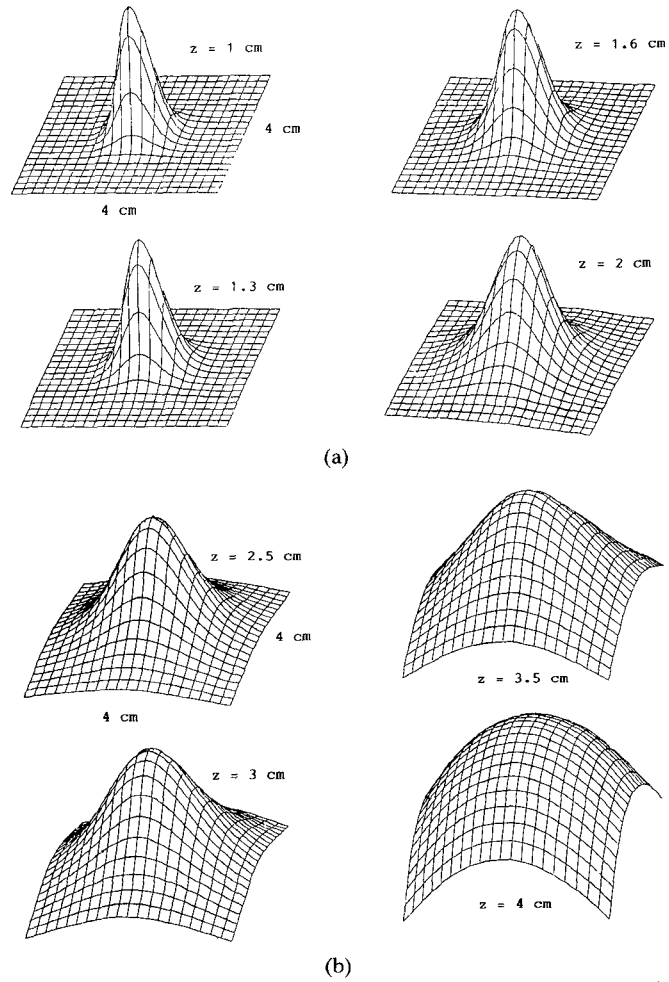


Fig. 6. Defocusing of the power deposition as a function of depth in the example of Fig. 4

from temperature measurements in a layered biological tissue heated by a waveguide applicator.

## VII. Conclusions

The use of (an array of) microstrip antennas in the local hyperthermia treatment of malignant tumors becomes increasingly important. To be able to predict the power deposition generated by this type of antennas, we started from a planar stratified model of a biological tissue. With the help of a suitable electric Green's dyadic an integral equation for the surface current density on the surface of the microstrip antenna could be formulated. To solve this integral equation, the method of moments was applied. A correct handling of the self-patch contribution was only possible starting from a thorough analytical knowledge of the behavior of the Green's dyadic. Special attention was paid to a correct modeling of the behavior of the current near the edges of the microstrip patch and near the feed point. The numerical results show that a strong defocusing of the dissipated power occurs at more than half a wavelength away from the antenna. In the future the proposed method will be extended to cover more complex geometries of the microstrip patches and the interaction between several antennas.

## REFERENCES


[1] J. James, P. Hall, and C. Wood, *Microstrip Antenna Theory and Design*. London: Peter Peregrinus, 1981.

[2] Y. Lin and L. Shafai, "Moment-method solution of the near-field distribution and far-field patterns of microstrip antennas," *Proc. Inst. Elec. Eng.*, vol. 132, pt. H, no. 6, pp. 369–374, Oct. 1985.

[3] Q. Zhang, Y. Fukuoka, and T. Itoh, "Analysis of a suspended patch antenna excited by an electromagnetically coupled inverted microstrip feed," *IEEE Trans. Antennas Propagat.*, vol. AP-33, pp. 895–899, 1985.

[4] P. Katehi and N. Alexopoulos, "On the modeling of electromagnetically coupled microstrip antennas—The printed dipole," *IEEE Trans. Antennas Propagat.*, vol. AP-32, pp. 1179–1186, 1984.

[5] M. Kominami, T. Takei, and K. Rokushima, "A printed dipole electromagnetically coupled to a microstrip line feed," in *Proc. of ISAP 1985*, pp. 93–96.

[6] A. Tulintseff, "Experiment and analysis of circularly polarized electromagnetically coupled microstrip antennas," presented at the 1986 National Radio Science Meeting, Boulder, CO, 1986.

[7] A. Das and S. Das, "Input impedance of a probe excited circular microstrip ring antenna," *Proc. Inst. Elec. Eng., pt. H*, vol. 132, pp. 384–390, 1985.

[8] L. Walters, "Rectangular ring and H-shaped microstrip antennas—Alternatives to rectangular patch antenna," *Electron. Lett.*, vol. 21, pp. 874–876, 1985.

[9] M. Mehler, T. Maclean, and A. Abbas, "Input impedance of a circular microstrip disc antenna using mode matching," *Electron. Lett.*, vol. 21, pp. 874–876, 1985.

[10] R. Johnson, G. Andrasic, D. Smith, and J. James, "Field penetration of arrays of compact applicators in localized hyperthermia," *Int. J. Hyperthermia*, vol. 1, pp. 321–336, 1985.

[11] J. Mosig and F. Gardiol, "General integral equation formulation for microstrip antennas and scatterers," *Proc. Inst. Elec. Eng.*, vol. 132, pt. H, no. 7, pp. 424–432, Dec. 1985.

[12] L. Beyne and D. De Zutter, "Green's function for layered lossy media with special application to microstrip antennas," submitted to *IEEE Trans. Microwave Theory Tech.*

[13] J. Van Bladel, "Field singularities at metal–dielectric wedges," *IEEE Trans. Antennas Propagat.*, vol. AP-33, pp. 450–455, 1985.

[14] F. Bardati, M. Mongiardo, D. Solimini, and P. Tognolatti, "Biological temperature retrieval by scanning radiometry," in *1986 IEEE MTT-S Int. Microwave Symp. Dig.*, pp. 763–766.


✠

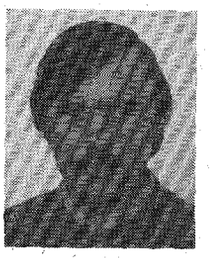

**Luc Beyne** was born in Ostend, Belgium, on July 1, 1963. He received the degree of electrical engineer (a five-year program equivalent to the M.S. degree) from the University of Ghent, Belgium, in 1986. At present he is with Alcatel Bell Telephone, Antwerp, Belgium, where he is engaged in broad-band ISDN research.

✠

**Daniel De Zutter** was born in Eeklo, Belgium, on November 8, 1953. He received the degree of electrical engineer (a five-year program equivalent to the M.S. degree) from the University of Ghent, Belgium, in 1976. From September 1976 to September 1984, he was a research and teaching assistant at the Laboratory of Electromagnetism and Acoustics of the University of Ghent. In October 1981 he obtained the Ph.D. degree from the same university and in April 1984 he completed a thesis leading to the "Aggregaat van het Hoger Onderwijs," a degree equivalent to the German "Habilitation" and the French "Agrégation."

Most of his scientific work up to 1984 dealt with the electrodynamics of moving media. In October 1984 he became a Research Associate with the National Fund for Scientific Research of Belgium. He is now engaged in hyperthermia research and in research on high-frequency microstrip interconnections.